Nov 24th, 12:00 AM

Design vs. Test Results for Steel Deck Floor Slabs

Max L. Porter

C. E. Ekberg Jr.

DESIGN VS. TEST RESULTS FOR STEEL DECK FLOOR SLABS

M. L. Porter[a] and C. E. Ekberg, Jr.[b]

INTRODUCTION

An extensive experimental and theoretical investigation of steel-deck-reinforced floor slabs was undertaken in 1967 at Iowa State University (ISU) under the sponsorship of the Ame an Iron and Steel Institute (AISI). To date, 353 full-scale specimens have been tested. See Ref. 3 for a summary of tests. An over-view of the types of specimens tested was presented at the First Specialty Conference on Cold-Formed Steel Structures [4]. The majority of tests have been one-way slab elements as shown in Fig. 1. The results of some of these full-scale experimental tests will be utilized in this paper for illustrating a comparison with design recommendations.

Design recommendations for steel-deck-reinforced floor slabs are contained in the latest American Iron and Steel Institute's draft entitled "Tentative Recommendations for the Design of Composite Steel Deck Slabs" and Commentary. Another paper by the same authors at this Third Specialty Conference presents some of these tentative design recommendations [5], and an additional paper by T. J. McCabe presents an example design utilizing the recommendations [2]. The purpose of this paper is to present results

[a]Assistant Professor, Civil Engineering Dept., Iowa State Univ., Ames, Iowa.
[b]Professor & Head, Civil Engineering Dept., Iowa State Univ., Ames, Iowa.

of the computations utilizing the design predictions recommended for the shear-bond capacity of steel deck slabs as compared with experimental data. In addition, end-slip and deflection behavioral characteristics associated with a shear-bond failure mode are presented.

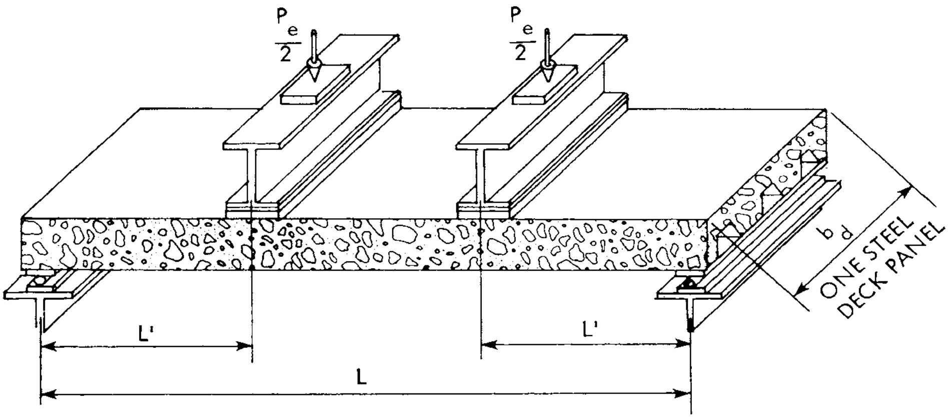

Fig. 1. Typical arrangement for testing one-way slab elements.

SHEAR-BOND END-SLIP BEHAVIOR

Most steel-deck-reinforced floor slabs fail by the shear-bond mode of failure. This failure mode is characterized by the formation of a diagonal tension crack in the concrete at or near one of the load points followed by end-slip at one end of a one-way slab element as described previously [5]. A photograph illustrating this displacement between the steel decking and concrete at one end-face is shown in Fig. 2. The shear-bond failure observed from the experimental tests was typically rather sudden, with the concrete moving horizontally, overriding or

Fig. 2. Photograph of end-slip after failure of a one-way slab element.

failing the shear transferring device, which consisted of embossments, spot-welded wires, or concrete protruding through holes in the steel deck.

Typical load-displacement relationships for end-slip are given in Fig. 3. Most steel deck systems do not experience end-slip until reaching the ultimate load, as illustrated by the relationship on the left in Fig. 3. However, some systems may experience end-slip prior to ultimate, as shown by the load-displacement plot on the right in Fig. 3.

Additional behavioral displacement information will be presented later in this paper.

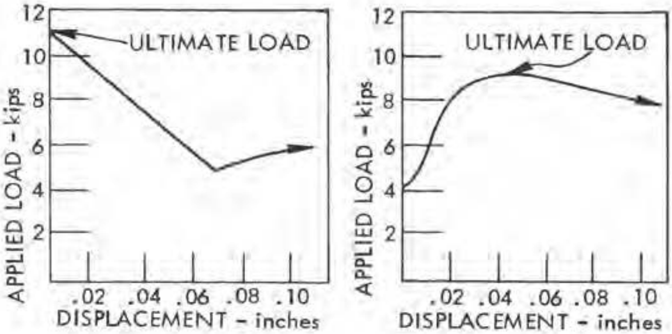

Fig. 3. Typical load-displacement relationships for end-slip.

SHEAR-BOND DESIGN FORMULATION

As previously described [5], a series of performance tests, like those in Fig. 1, is necessary to properly establish a relationship for strength involving significant parameters affecting the shear-bond capacity. Since the above described slippage between the concrete and the steel deck occurs along the region of the shear-span length, L', as shown in Fig. 1, a primary parameter for shear-bond computation is L'. Other important parameters include the following:

1. ultimate experimental end shear, $V_e = P_e/2bd$;
2. reinforcement percentage, $\rho = A_s/bd$;
3. cross-sectional area of steel deck, A_s;
4. concrete strength, f'_c;
5. specimen width, b, and effective depth, d; and
6. center-to-center spacing of shear transferring devices, s, where such devices are variable from one deck section to another, such as holes or transverse wires. For those devices having a fixed pattern, such as embossments, s is taken as unity.

Utilizing the shear formulation as contained in the ACI Building Code [1], the above parameters can be combined to form the terms $V_e s/bd\sqrt{f'_c}$ and $\rho d/L'\sqrt{f'_c}$, plotted as y- and x-coordinates, respectively, for the performance test series as demonstrated in Fig. 4. To obtain the necessary strength relationship, a linear regression is obtained for the plotted points. To account for differences between field conditions and

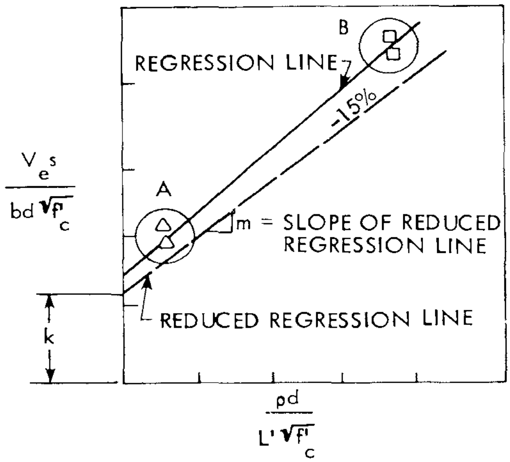

Fig. 4. Relationship between $\frac{V_e s}{bd\sqrt{f'_c}}$ and $\frac{\rho d}{L'\sqrt{f'_c}}$.

those in the laboratory, the regression line is reduced by -15 percent to obtain the design slope, m, and intercept, k. Thus the computed shear-bond capacity, V_u, is found from

$$\frac{V_u s}{bd\sqrt{f'_c}} = \frac{m\rho d}{L\sqrt{f'_c}} + k \tag{1}$$

where the non-reduced value of the slope of the regression line is given by

$$m = \frac{n\Sigma XY - \Sigma X \Sigma Y}{n\Sigma X^2 - (\Sigma X)^2}$$

and the non-reduced value of the regression line intercept is given by

$$k = \frac{\Sigma Y \Sigma X^2 - \Sigma X \Sigma XY}{n\Sigma X^2 - (\Sigma X)^2}$$

Equation (1) has been found to be valid for all the various means of shear transfer for steel decks currently manufactured. Since each steel deck configuration has a different regression plot, a separate determination of m and k in Eq. (1) is a necessity for each different steel deck cross section.

Examples of the plot from Fig. 4. for Eq. (1), utilizing strength data from tests of slabs constructed with various deck types, are shown in Figs. 5-8. Each of these figures represents a linear regression for a different steel deck type. Lines representing plus or minus 15 percent deviation intervals from the regression line are shown as an aid in determining the spread of the data. Figures 5-8 are representative of results obtained from Eq. (1) and provide a quantitative measure of the accuaracy of this equation in predicting the ultimate shear force for slab elements where the shear-bond mode of failure governs.

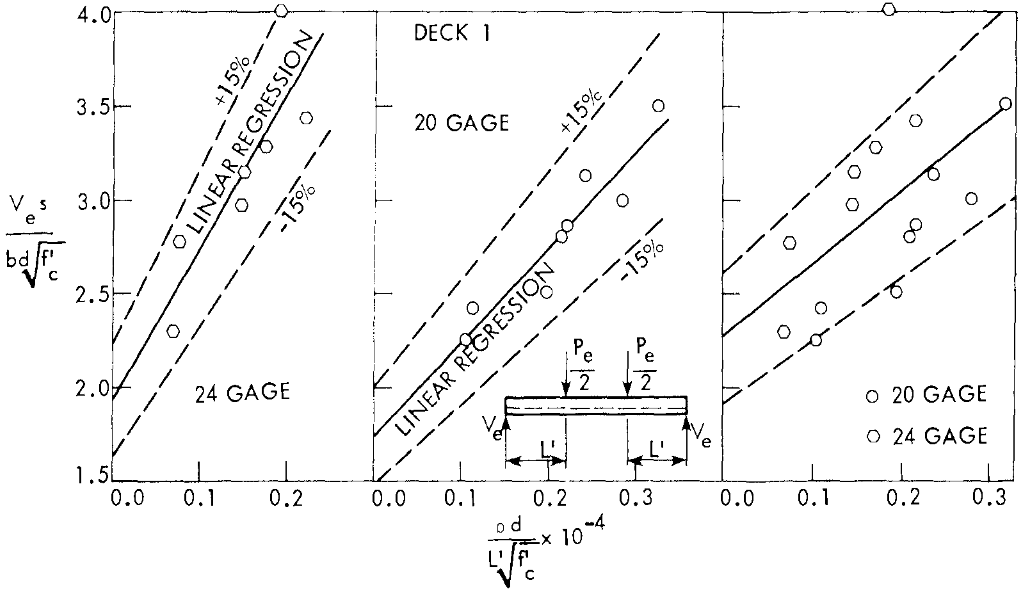

Fig. 5. Example shear-bond regression for deck type 1.

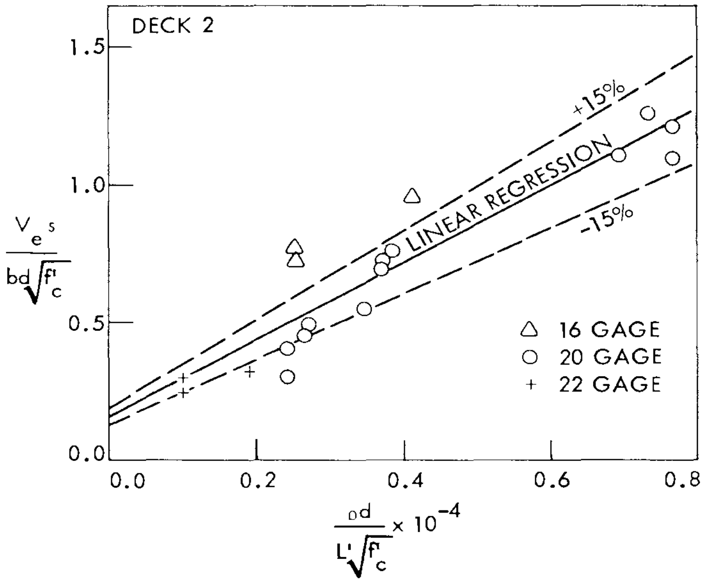

Fig. 6. Example shear-bond regression for deck type 2.

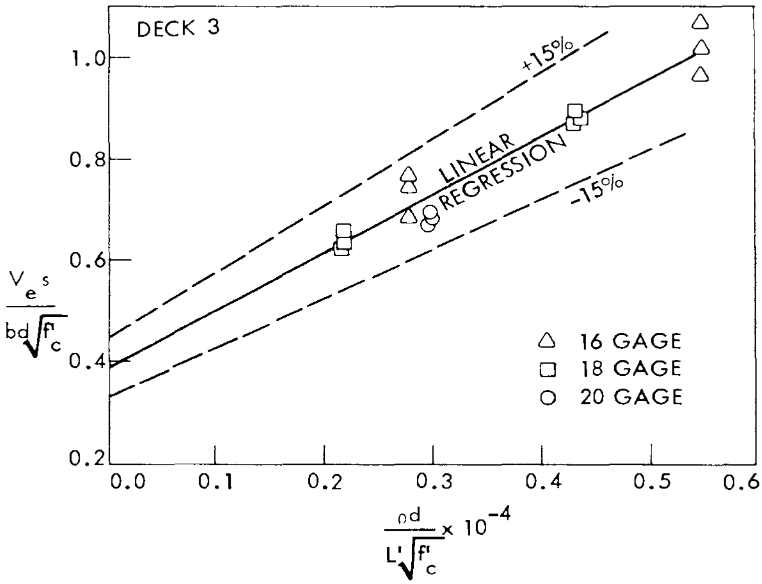

Fig. 7. Example shear-bond regression for deck type 3.

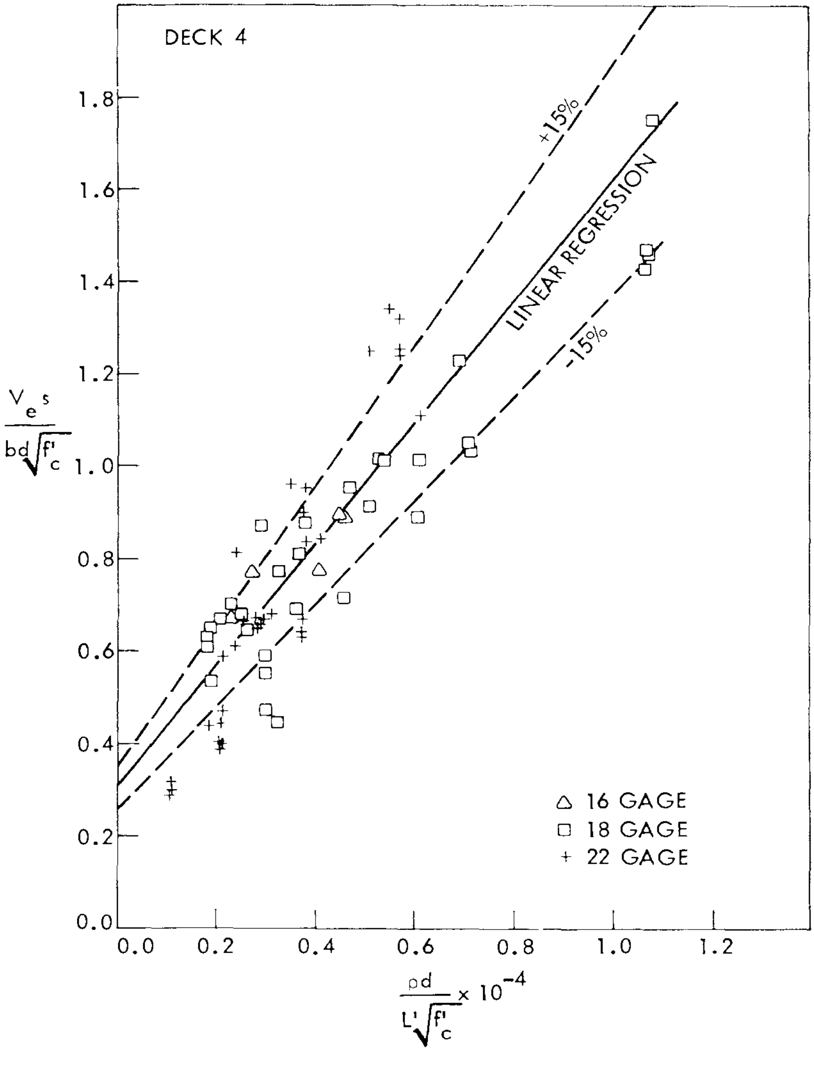

Fig. 8. Example shear-bond regression for deck type 4.

In some instances, a significantly different equation determination can be made for each gage thickness of the same steel deck cross section. The diagrams in Fig. 5 indicate there is a definite change in the regression constants m and k as gage thickness changes. A composite diagram shown in Fig. 5(c) illustrates a much greater scatter for a regression of the combined gage thickness. This greater scatter (to a lesser degree) is illustrated in Figs. 6 and 8. Figure 7 indicates little or no influence of gage thickness on the constants m and k. For those steel decks where gage thickness significantly influences the regression constants m and k, separate equation determinations should be made for each gage thickness to more accurately predict the ultimate shear capacity.

In addition to the steel deck configuration and gage thickness, a separate regression equation determination may be needed for other significant variables not accounted for in Eq. (1). For example, the shear-bond capacity is dependent upon the surface coating of the steel deck. If more than one coating is used, then an additional equation determination is necessary unless the m and k constants for the more conservative (lower) shear values are used. An additional example of where a separate determination may be needed is for lightweight versus normal weight concretes, unless the more conservative results are used for both concrete types.

SHEAR-BOND DESIGN EQUATIONS

As previously described [5], Eq. (1) can be re-written for design in the following form to give the calculated ultimate shear, V_u in pounds per foot of width:

$$V_u = \phi \left[\frac{12d}{s} \left(\frac{m\rho d}{L'} + k\sqrt{f'_c} \right) + \frac{\gamma W_1 L}{2} \right] \qquad (2)$$

where ϕ = shear-bond capacity reduction factor = 0.80

γ = portion of dead load added upon removal of shear, see Ref. 2

W_1 = slab dead load, psf

Utilizing the load factors in the ACI Building Code [1], the allowable superimposed live load (LL) in pounds per square foot is:

$$LL = \frac{1}{1.7} \left[\frac{2V_u}{L} - 1.4 \ (\gamma W_1 + W_3) \right] \qquad (3)$$

where L = span length, feet

W_3 = dead load applied to slab exclusive of W_1, psf.

EXAMPLE RESULTS OF SHEAR-BOND PREDICTIONS

Based upon design Eqs. (2) and (3), several illustrative examples will be presented. As a means of indicating the validity of the predicted results, the experimental load-deflection relationships for slab elements constructed with 16, 18, and 20 gage deck will be utilized. See Figs. 9 and 10. The experimental deflections were measured at midspan and represent the maximum vertical displacement at each applied loading increment. Indicated on each curve is a horizontal line corresponding to the allowable live load (ALLOW LL) as obtained from Eq. (3). The constants m and k in Eq. (2) were obtained from linear regressions shown in Fig. 11, where data from tests on slab elements is plotted separately according to gage thickness. All specimens in Figs. 9-11 were reinforced with a

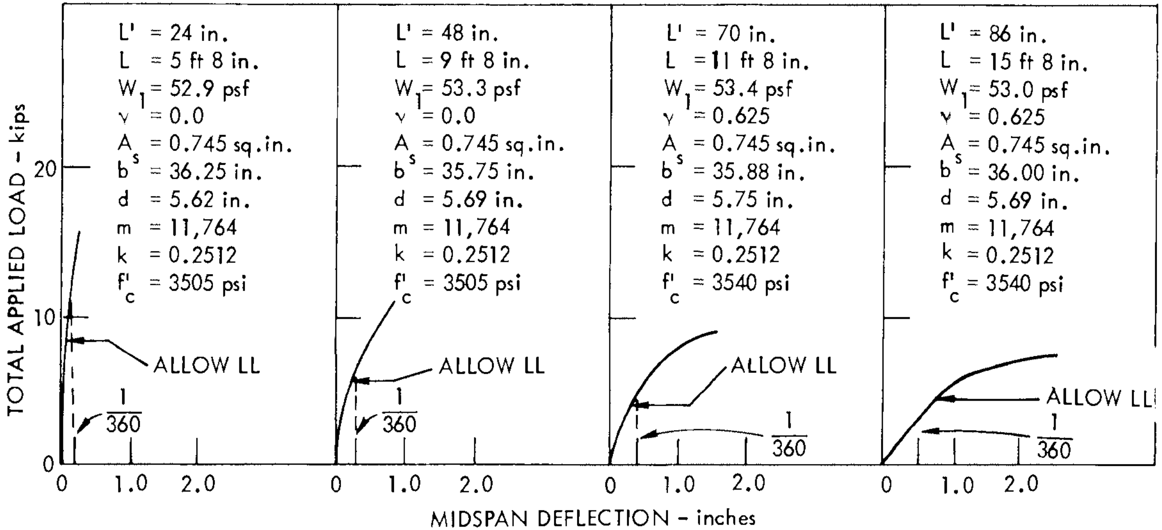

Fig. 9. Example load-deflection relationships of various shear spans and span lengths showing the allowable live load for specimens reinforced with 18 gage steel deck.

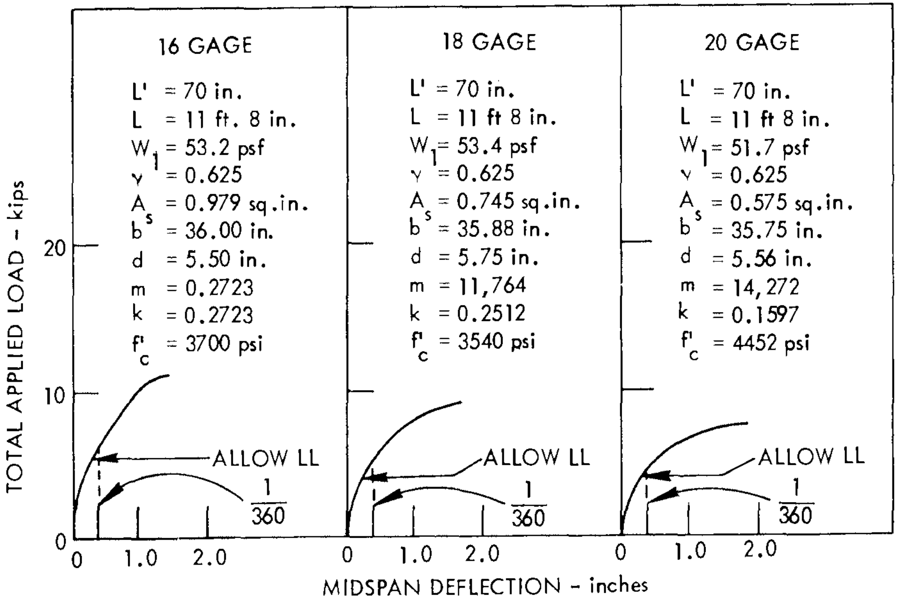

Fig. 10. Example load deflection relationships showing the effects of specimens reinforced with different gage thicknesses of steel deck.

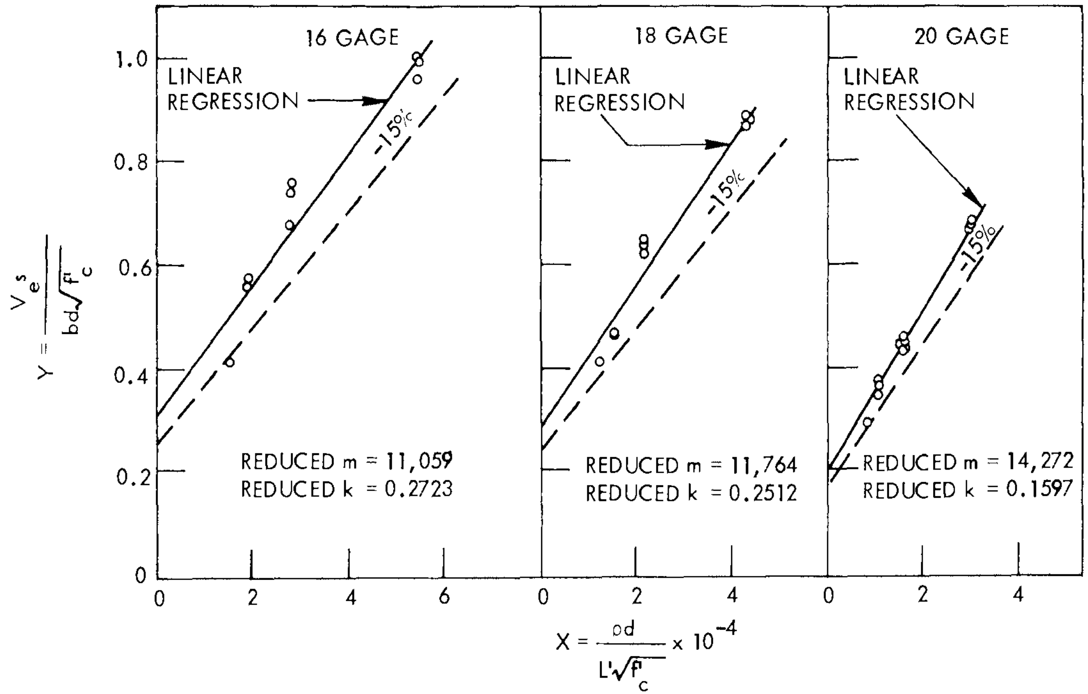

Fig. 11. Linear regression relationships for obtaining design live loads indicated in Figs. 9 and 10.

three-inch deep steel deck having embossments as the means of shear transfer between the deck and concrete. The nominal width and out-to-out depth of all specimens was 36 in. by 5-1/2 in. and the lengths varied from 6 to 16 feet. The concrete had an average compressive strength of approximately 4,000 psi. Other pertinent data used in Eqs. (2) and (3) is indicated in Figs. 9-11.

As can be seen, each of the predicted allowable live load values in Figs. 9 and 10 falls just above the upper limit of the straight-line portion of the load-deflection curves. Thus, the computed live load in all cases provides good results in comparison to the ultimate and behavioral test data and provides a consistant and reasonable margin of safety for all the test members.

Figure 9 gives examples of load-deflection behavior for specimens reinforced with the same gage thickness of steel deck, but with varying shear spans and span lengths. It is evident that the behavior changes considerably from a short shear span to a long shear span. The slab elements exhibit considerable stiffness with little nonlinearity when the shear-span is short. However, the long shear-span (and span length) induces much more ductility and considerable nonlinearity. It is significant that the computer allowable live load (ALLOW LL) provides consistent results for each type of load-deflection relationship, i.e., decreasing load with increasing shear span and span length.

Figure 10 gives load-deflection relationships for specimens reinforced with three different gage thicknesses of steel deck, but having the same shear span and span length. As expected, the ultimate load decreases with decreasing thickness of steel deck reinforcing. Also, the nonlinearity increases slightly with decreasing thickness of the steel. Again, it is significant that the predicted live load provides consistent results, i.e. decreasing load with decreasing steel thickness.

Figures 9 and 10 include a vertical line indicating the allowable deflection limitation of $\frac{1}{360}$ of the span length. As can be seen the load-deflection behavior is a fairly straight-line relation to the left of this allowable deflection limitation. In addition, the $\frac{1}{360}$ of the span length limitation is significant in comparison with the computed allowable live load. In most cases the allowable LL value was close to or within the $\frac{1}{360}$ limitation, indicating somewhat of a "balanced" design with respect to deflections.

CONCLUSIONS

1. All simple span slab elements failing by a shear-bond mode of failure exhibit end-slip between the steel deck and concrete.

2. Most steel-deck-reinforced slab systems exhibit end-slip upon reaching the ultimate failure load.

3. Plots of the terms $V_e s/bd\sqrt{f'_c}$ and $\rho d/L'\sqrt{f'_c}$ give consistent and reasonable linear regression relationships from which a design equation can be written for predicting the maximum load for shear-bond.

4. On the basis of load-deflection data, it is apparent that the recommended design equations for shear-bond provide a consistent margin of safety.

ACKNOWLEDGMENTS

The proposed design criteria presented in this paper are part of the American Iron and Steel Institute's (AISI) latest draft of "Tentative Recommendations for the Design of Composite Steel Deck Slabs and Commentary." The design criteria is based upon an extensive theoretical and experimental research program sponsored by AISI and conducted by the Engineering Research Institute of Iowa State University. Valuable guidance in the conduct of the research was provided by the AISI's Task Committee on Composite Construction of the Joint Engineering Subcommittee of the Committees of Hot Rolled and Cold Rolled Sheet and Strip Producers and Galvanized Sheet Producers under chairmanship of Mr. T. J. McCabe and past chairman Mr. A. J. Oudheusden.

REFERENCES

1. American Concrete Institute, Building Code Requirements for Reinforced Concrete (ACI 318-71). Detroit, Michigan: American Concrete Institute, 1971.

2. McCabe, T. J., "Design Example of Steel Deck Reinforced Floor Slabs," Proceedings of Third Specialty Conference of Cold-Formed Steel Structures, Dept. of Civil Engineering, University of Missouri-Rolla, November 1975.

3. Porter, M. L., and Ekberg, C. E., Jr., Discussion of paper by the Subcommittee on the State-of-the-Art Survey of the Task Committee on Composite Construction of the Committee on Metals of the Structural Division entitled "Composite Steel-Concrete Construction," ASCE Journal of the Structural Division, Vol. 101, No. ST3, March 1975.

4. Porter, M. L., and Ekberg, C. E., Jr., "Investigation of Cold-Formed Steel-Deck-Reinforced Concrete Floor Slabs," Proceedings of First Specialty Conference on Cold-Formed Steel Structures, Dept. of Civil Engineering, University of Missouri-Rolla, August 19-20, 1971.

5. Porter, M. L., and Ekberg, C. E., Jr., "Tentative Design Recommendations for Steel Deck Reinforced Floor Slabs," Proceedings of Third Specialty Conference on Cold-Formed Steel Structures, Dept. of Civil Engineering, University of Missouri-Rolla, November 1975.

APPENDIX - NOTATION

A_s Cross-sectional area of steel deck where used as tension reinforcement, in.^{2}/ft of width

b Width of slab

d Effective slab depth (distance from extreme concrete compression fiber to centroidal axis of the full cross-sectional area of the steel deck), in.

f'_c 28-day compressive test cylinder strength, psi

k Intercept of regression line

L Length of span, ft.

LL Allowable superimposed live load for service conditions, psf

L' Length of shear span, in.

m Slope of regression line

s Center-to-center spacing of shear transfer devices other than embossments, in.

V_u Calculated ultimate shear based on shear-bond failure, lb/ft of width

W_1 Weight of slab (concrete plus steel deck), psf

W_3 Dead load applied to slab, exclusive of W_1, psf

γ Coefficient depending on support during curing

ϕ Capacity reduction factor

ρ Reinforcement ratio, A_s/bd